European Battery, Hybrid and Fuel Cell Electric Vehicle Congress
Geneva, 14th - 16th March 2017

A Comparative Study on Different Cooling Strategies for Lithium-Ion Battery Cells

Elham Hosseinzadeh [1], Anup Barai [1], James Marco [1], Paul Jennings [1]
[1]*WMG-University of Warwick, Coventry, UK, e.hosseinzadeh@warwick.ac.uk*

Abstract

In this study a 1D electrochemical-thermal model is coupled with a 3D thermal model in order to predict the heat generation and corresponding temperature distribution in a battery cell. The developed model is verified against experimental data for a 20 Ah lithium iron phosphate (LFP) which is operating at 20 °C ambient temperature. The model is then adjusted to accommodate for 10Ah and 40 Ah cells by decreasing and increasing the surface area of each cell as well as the tab dimensions. The temperature distribution of the different cells are studied employing fin cooling as well as indirect liquid cooling system. Simulation results highlight that the temperature gradient within the surface of the 40 Ah cell is almost 1.9 and 1.3 times that of the 10 Ah and 20 Ah cells, respectively. Moreover, it is found that the fin cooling method by employing aluminium plates between the cells is not a good choice when applied to large format batteries. Whereas, by employing the indirect liquid cooling, a very uniform temperature along with low temperature gradient is achieved even under high discharge rate. When the two cooling units have the same volume, the obtained volumetric temperature gradient with fin cooling is equal to 20.5, 27.5 and 34.7 °C for the 10 Ah, 20 Ah and 40Ah respectively, whereas the corresponding value in case of the indirect cooling is 4.7, 5.2 and 6.2 °C respectively.

Keywords: Lithium ion batteries, Thermal management, Electrochemical-thermal model, 3D modelling

1 Introduction

Lithium ion batteries have an optimum range of operating temperature (15-35 °C), within which they have the best performance [1], [2]. In addition, the temperature gradient of the battery in both the cell level and pack level should be kept lower than 5 °C to reduce the degradation rate[2-4]. Battery characteristics such as power and energy density, cycle life, reliability and cost are strongly affected by their operating temperature. Therefore, a proper thermal management system is required to ensure a safe operation as well as prolonged lifetime. Designing a thermal management system depends on many factors such as the size of the battery, operating conditions, energy capacity and power requirement of the pack as well as the pack configuration [5].

The main duties of a battery thermal management system are to minimise the impact of hot or cold external ambient conditions on the battery pack, minimise the temperature gradient between and within the single cells, prevent risk of uncontrolled cell temperatures and cell-to-cell propagation of thermal runaway. It should also safely prevent any

condensation within the battery pack resulting from uncontrolled humidity [6].

Common thermal management methods are air cooling [7-13], liquid cooling [5], [14] and fin cooling [1]. Heat pipe [3], [15-17] and phase change material (PCM) [18-20] are other alternatives for battery cooling. Generally active air cooling system consumes the most parasitic power among the other cooling methods [1]. It is applicable to battery systems with low heat generation per cell ($Q_{cell} < 10\ W$) [5]. Moreover, the capacity of the air cooling system is dependent on the ambient conditions, and it may cause a large non-uniform temperature distribution during aggressive drive cycles [21], [22]. Liquid cooling adds more cost, weight and complexity to the system compared to air cooled systems [23]. The cooling plate itself is expensive and it needs to be properly designed. Moreover, auxiliary components such as heat exchanger, pump and so on, adds weight and complexity to the system. On the other hand, it offers a higher cooling capacity which makes it desirable for electric vehicle application [17], [18]. The advantages of heat pipes over the other cooling methods are their high thermal conductivity, compact structure and flexible geometry [3]. However, the effectiveness of such cooling systems can still be greatly improved.

To design a thermal management system for electric vehicles (EV) or hybrid electric vehicles (HEV) the trade-off between efficiency, cost and weight should be considered. In order to evaluate the existing trade-off, fin cooling and indirect liquid cooling systems are employed and investigated for different cells individually. The objective is to identify the optimal design, in terms of temperature distribution, size and complexity of the cooling system. Hence, in this study primarily impact of battery dimensions, battery capacity, and their combined interplay on the overall heat generation and corresponding temperature distribution of a battery cell is investigated. Further, the thermal behavior of the three different cells, 10 Ah, 20 Ah and 40, employing fin cooling and indirect liquid cooling systems is studied and compared.

2 Methodology

The focus of this study is to find the optimal cell size for the battery pack considering the heat generation and temperature distribution, volume of the pack and design of the cooling system. To achieve the objectives of this study, in the first step a battery model is developed to predict the heat generation as well as the temperature distribution of the cell. The model combines a 1D electrochemical-thermal calculation for one electrode pair with a 3D thermal calculation of a cell sequentially in order to capture the temperature distribution at the cell scale. In essence the 1D electrochemical-thermal model provides a heat source (generated heat from a constant charge/discharge cycle or a drive cycle) for the 3D thermal model in the cell level. The inputs to this model are current, capacity, geometrical design, material properties and ambient temperature, while the outputs are the responses of the cell to the current load, i.e. voltage, generated heat, temperature profile across the cell surface, state of charge and all other internal variables that are key for the successful operation and durability of the cell. The anode is made of graphite and the cathode material is lithium iron phosphate (LFP). The model is verified against experimental data for a 20Ah pouch cell which is operating at 20°C ambient temperature with different C-rates (1C,3C, 5C). The model is developed in a way that can be adjusted for different kind of cells with different chemistries, once the physical and thermal parameters of the cell are known. The battery cells in this study are 10 Ah, 20 Ah and 40 Ah LFP pouch cells. The batteries have similar electrochemical characteristics, such as electrode thickness, particle size, porosity, but they are different in surface area ($H_{cell} \times W_{cell}$) and tab width (W_{tab}), as shown in Fig. 1. The geometrical dimensions of different cases are summarised in Table 1.

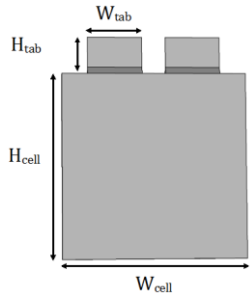

Figure 1. Geometrical configuration of a LFP pouch cell.

Table 1. Physical dimensions of LFP pouch cells for different cases.

Cell (Ah)	H_{cell} (mm)	W_{cell} (mm)	W_{tab} (mm)	H_{tab} (mm)	Thickness (mm)
10	135	135	40	30	7.5
20	190	190	60	30	7.5
40	270	270	90	30	7.5

3 Results and discussion

3.1 Model Validation

A 1D electrochemical-thermal model is coupled with a 3D thermal model in order to predict the heat generation and corresponding temperature distribution in a battery cell. The model is validated against a 20 Ah LiFePO4 pouch cell subject to 1C, 3C and 5C continuous discharge conditions [24]. The cell is placed in a climate chamber at 20 ℃ while the two sides of the cell are exposed to the air. A free convection boundary condition with h value of ($h = 10\, Wm^{-2}.K$), is considered around the cell surface [24]. The surface temperature of the cell is measured by seven thermocouples place on both sides. The validation of the 3D thermal model is presented in Figure 2. The comparison is made for the maximum surface temperature obtained through the 3D model versus the measured temperature through the experiments for the 1C, 3C and 5C constant discharge rate. The peak error of the simulation results at 1C, 3C and 5C is equal to 10.6%, 10.2% and 10.4% respectively. The error can be attributed to the assumption of the constant h-value as well as inaccuracy of the temperature dependent electrochemical parameters.

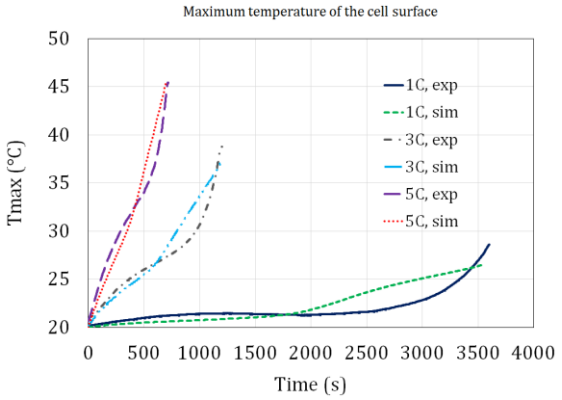

Figure 2. Maximum cell surface temperature of the 20Ah LFP pouch cell at 20 °C, with natural cooling condition.

By operating the batteries under a constant 3C and 5C discharge rate at 20°C ambient temperature the following results are obtained. Table 2 summarises the average, maximum and minimum volumetric temperatures of the batteries at the end of 3C and 5C discharge along with the time averaged heat generation. The cells are fully insulated, meaning that there is no convective flux around the cells, and heat transfer coefficient is equal to zero ($h = 0$).

Table 2. Heat generation and temperature profile of different cells – Reference Cases

Cell (Ah)		Q_{cell} (W)	T_{ave} (°C)	T_{max} (°C)	T_{min} (°C)	ΔT_{surf} (°C)
10	3C	7.5	49	49.1	48.8	32.15
	5C	17.2	58.3	59.0	58.1	0.9
20	3C	15	49.4	50.1	49.1	1.0
	5C	34.3	58.9	61.5	58.1	3.4
40	3C	29.9	49.8	52.4	49	3.4
	5C	69.7	59.6	66.7	57.9	8.8

Employing Large format batteries lead to a more compact pack with less wiring and connections, so they are preferred from this point of view. On the other hand, they have a larger temperature gradient within the surface of the battery, which makes the thermal management very challenging, as displayed in Table 2. In this study, fin cooling and indirect liquid cooling systems are applied on the surface of the cells to identify the pros and cons of large format compared to small format batteries.

3.2 Fin Cooling

The primary cooling unit contains aluminium plates inserted between the cells which act as a heat sink. By imposing a constant temperature at the edge of the plates, $T = 20°C$, the following temperature profiles within the battery cells are achieved, as depicted in Figure 3(a,b,c).

The average and maximum temperature of the cells at the end of 3C and 5C discharge are summarised in Table 3. As seen by employing aluminium plates between the cells of different capacities, different temperature profiles achieved. Under a constant 5C discharge rate, the temperature gradient within the surface of the 40 Ah cell is almost 1.7 and 1.3 times that of the 10 Ah and 20 Ah cells, respectively. Even for the 10 Ah the temperature gradient is quite high, 20.5°C, indicating that this cooling method is not very efficient for cells operating under 5C discharge rate. However, by operating the cell at 3C instead of 5C the temperature gradient reduces significantly, by 41%, 37% and 34% for the 10 Ah, 20 Ah and 40 Ah cell respectively. Moreover, the average volumetric temperature of the cells reaches to 29.1, 32.9 and 36.4 which is within the optimal operating temperature of the cells. The temperature evolution of the cells over the time under a constant 3C and 5C discharge are shown in Figure 4.

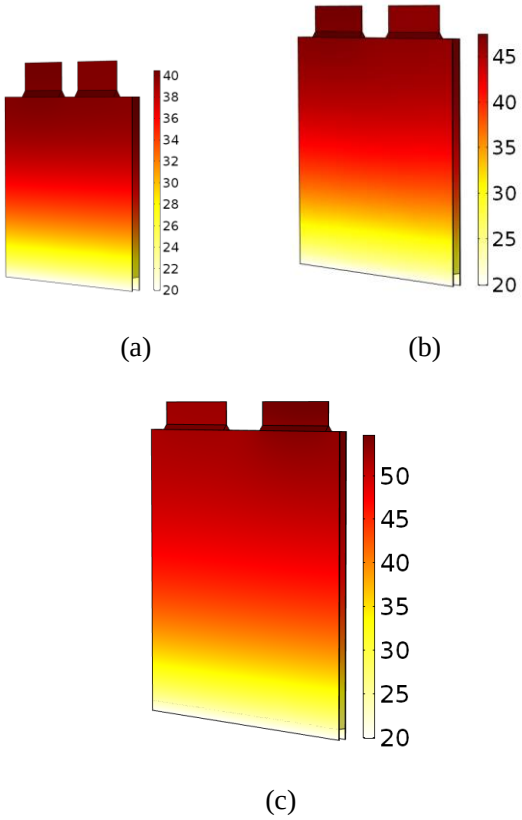

Figure 3. Temperature distribution of the batteries by applying fin cooling, inserting aluminium plates between the cells for, (a) 10 Ah, (b) 20 Ah, (c) 40 Ah battery cells.

Table 3. The average and maximum volumetric temperature as well as the temperature gradient values of the different cells at the end of 3C and 5C discharge, applying fin cooling, the thickness of the aluminium plate is ($t_{Al} = 1.5\ mm$).

Cell (Ah)		T_{ave} (°C)	T_{max} (°C)	ΔT (°C)
10	3C	29.1	31.2	12.1
	5C	35.3	40.5	20.5
20	3C	32.9	37.3	17.3
	5C	40.3	47.5	27.5
40	3C	36.4	42.9	22.9
	5C	44.3	54.7	34.7

In order to decrease the temperature gradient of the cells a thicker aluminium plate with $t_{Al} = 5\ mm$ was embedded between the cells. The simulation results are summarised in Table 4. By increasing the plate thickness from 1.5 to 5 mm, the temperature gradient of the 10 Ah, 20 Ah and 40 Ah reached to 9.6, 14.1 and 18.3 °C at the end of 5C discharge, whereas at the end of 3C discharge a temperature gradient of 5.3, 8.4, 11.9 °C was achieved.

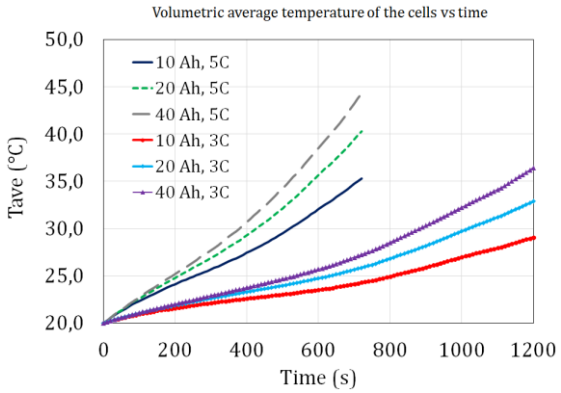

Figure 4. The average volumetric temperature of the cells operating at 3C and 5C discharge rate at 20°C ambient temperature.

It is clear that the indirect cooling method by employing aluminium plates between the cells is not a good option when having large format batteries. However, another alternative, indirect liquid cooling is introduced in order to reduce the temperature gradient and to improve the thermal management of the batteries.

Table 4. The average and maximum volumetric temperature as well as the temperature gradient values of the different cells applying aluminium plates between the cells at the end of 3C and 5C discharge, the thickness of aluminium plate is ($t_{Al} = 5\ mm$).

Cell (Ah)		T_{ave} (°C)	T_{max} (°C)	ΔT (°C)
10	3C	23.7	25.3	5.3
	5C	26.7	29.6	9.6
20	3C	25.9	28.4	8.4
	5C	30	34.1	14.1
40	3C	28.5	31.9	11.9
	5C	33.3	38.3	18.3

3.3 Indirect Liquid Cooling

The second cooling method is indirect liquid cooling which comprises of aluminium cooling plates with embedded cooling channels. In order for the cooling methods to be comparable, both cooling units applied in this study have similar volume. The dimensions of the cooling plate is presented in Table 5. w_{ch} is the width of one channel, h_{ch} represents the thickness of the channels, and t_{Al} is the thickness of Al plate at each side of the channels. The volumetric temperature rise and the temperature gradient during a constant 3C and 5C discharge was investigated. Water/Glycol 50%

mixture as well as mineral oil were applied for cooling. The velocity range for water/Glycol mixture is 0.1-0.5 m/s to ensure a laminar flow regime approximation is valid.

Table 5. Dimensions of the cooling plates

	w_{ch} (mm)	h_{ch} (mm)	l_{ch} (m)	t_{Al} (mm)
10 Ah	10	1	0.51	0.25
20 Ah	7	1	0.73	0.25
40 Ah	5	1	1.00	0.25

Figure 5 presents the volumetric temperature gradient (ΔT) of the 40 Ah cell during a constant 5C discharge. By increasing the flow rate from 0.1 m/s to 0.5 m/s, ΔT is reduced by 49%. However the decreased rate is not proportional with the flow speed. For example by increasing the velocity from 0.3 to 0.5 m/s, ΔT is only reduced by 14%. It indicates that the gained cooling effect at high flow rates is not significant, whereas the parasitic power consumption of the pump increases dramatically as stated by:

$$P_{pump} = \sum_{i=1}^{n} \Delta P_i V_i \quad (1)$$

where ΔP_i is the total pressure drop in one cooling channel and i indicates the number of channels. V_i is the volumetric flow rate in the cooling channel. A similar trend is observed for volumetric temperature gradient of the 10 Ah and 20 Ah cell with different flow rates. For V=0.5 m/s the minimum ΔT at the end of discharge is approximately 6.2°C, whereas it can reduce to 5.1 and 4.7 for the 20 Ah and 10 Ah cells respectively. In case of applying mineral oil as coolant with velocity of 0.1 m/s, the ΔT of 15.3 °C is achieved at the end of 5C discharge, which is fairly high, almost twice of the gradient obtained through water mixture cooling. The limiting factor in case of oil cooling is the very high pressure drop in the channels. It means that even though the flow is within the laminar regime, the flow rate cannot increase any further because the power consumption of the pump dramatically increases as shown in Figure 6.

For identical flow rates, the pressure drop of the mineral oil is far more that of the water/glycol mixture. The difference is more pronounced as the flow rate increases. For example at V=0.1 m/s, ΔP of the mineral oil is 645 mbar whereas it is equal to 35 for the water/glycol mixture. While at V=0.5 m/s, ΔP is equal to 3233 mbar and 185 mbar for mineral oil and water/glycol mixture respectively. It highlights that in order to have a more efficient oil cooling system, a higher number of channels in parallel is required in order to reduce the pressure drop.

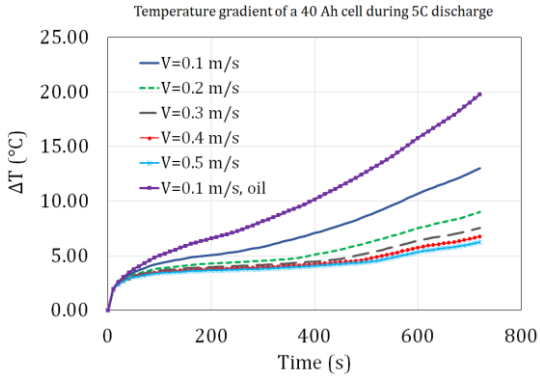

Figure 5. Volumetric temperature gradient of a 40 Ah pouch cell operating under 5C discharge rate at 20°C ambient temperature.

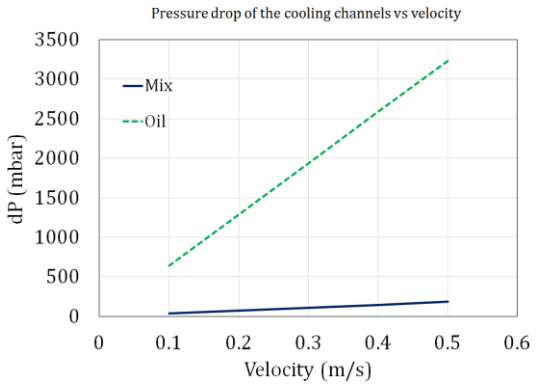

Figure 6. Pressure drop of the water/glycol mixture versus mineral oil for different flow rates.

The volumetric temperature gradient of the cells under 3C constant discharge is shown in Figure 7. As seen ΔT profile for the 10 Ah and 20 Ah and 40 Ah cell over the discharge process is quite similar. The volumetric ΔT at the end of discharge for a 10 Ah, 20 Ah and 40 Ah is equal to 2.5, 2.7, 3.3 °C respectively, showing a linear progression versus capacity of the cell.

The average volumetric temperature of the cell is as important as the volumetric temperature gradient. In a proper thermal management system, it is aimed to reduce both of those at the same time. The volumetric average temperature of the cells over the time under the constant 3C and 5C discharge condition is presented in Figure 8. At the end of a constant 3C discharge the average temperature of the 10 Ah, 20 Ah and 40 Ah increases by only 1.4, 1.5 and 1.8 °C respectively. Likewise, during the 5C

discharge it reaches to 2.6, 2.9 and 3.5 °C which is within the optimal range of the operating temperature. This proves the effectiveness of the indirect cooling channels with water/glycol mixture as the coolant.

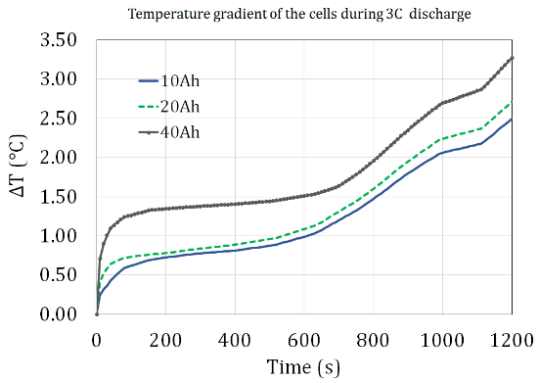

Figure 7. Volumetric temperature gradient of the 10 Ah, 20 Ah and 40 Ah cells during a 3C constant discharge rate at 20°C ambient temperature. The water/glycol velocity is equal to V=0.5 m/s for all the cases.

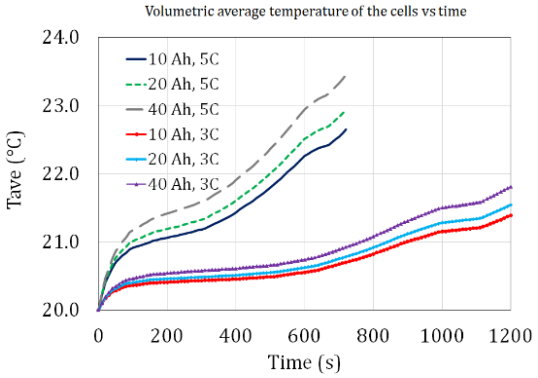

Figure 8. Volumetric average temperature of the 10 Ah, 20 Ah and 40 Ah cells over the time under 3C and 5C constant discharge at 20°C ambient temperature. The water/glycol velocity is equal to V=0.5 m/s for all the cases.

Similar study was conducted for a 40 Ah cell at 30 °C ambient temperature, as shown in Figure 9 and Figure 10. The inlet temperature of the coolant was set to both 20 °C and 30 °C. The time averaged heat generation of the cell at 20 °C and 30 °C under a constant 5C discharge is equal to 69.7 W and 51.7 W respectively. Under the 5C discharge, operating at 20 °C, the average temperature of 23.5 °C is achieved. At 30 °C, for $T_{coolant} = 20\,°C$, the average temperature starts to decrease from 30 °C to 21.4 °C until t=200 s, and then it starts increasing again until it reaches to 23.1 °C at the end of discharge. The lower temperature rise can be attributed to the lower value of the heat generation at the higher ambient temperature. Even though the time averaged temperature for the two cases is not identical, but after 200s they follow the same trend.

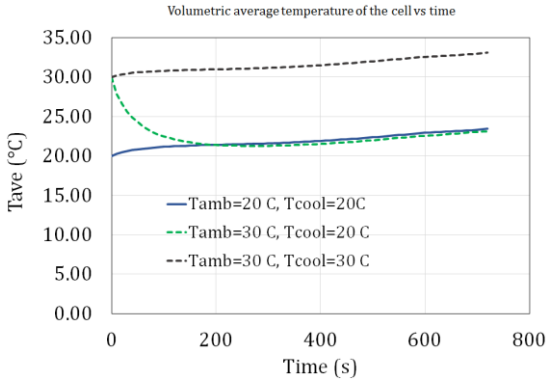

Figure 9. Average volumetric temperature of the 40 Ah cell at 20 °C and 30 °C ambient temperature. The water/glycol velocity is equal to V=0.5 m/s for all the cases.

In case of cell operation at 30 °C ambient temperature, and for $T_{coolant} = 30\,°C$, the cell operates at a higher temperature range, however the temperature rise is equal to 3.1°C, which is similar to the case with $T_{coolant} = 20\,°C$. Comparing the temperature gradient under different temperature conditions it is observed that, ΔT of the cell at the end of discharge under $20\,°C$ ambient temperature is 6.2 $°C$, whereas it is slightly lower at $30\,°C$ ambient temperature, which is 5.7 $°C$ and 5.6 $°C$, for $T_{coolant} = 20\,°C$ and $T_{coolant} = 30\,°C$, respectively.

The temperature distribution of the 40 Ah cell at the end of 5C discharge is presented in Figure 11. It is seen that the temperature profile of the cell across the surface is quite uniform with the approximate temperature gradient of 2°C whereas the temperature gradient through the thickness of the cell is much higher, as shown in Figure 12(a,b).(a)

(b)

Figure 12(a) presents the temperature gradient through the thickness of the cell while the cell is insulated. For this case, the gradient across the cell surface is equal to 8.8°C, whereas a gradient of 6.2°C is achieved through the thickness. By applying the indirect cooling, even though the temperature gradient across the surface reduces significantly, by approximately 6.8°C, but the gradient through the thickness doesn't change much. It reduces only by 16% which is equal to 1°C. It highlights that the most important limiting factor for reducing the volumetric temperature gradient of the cell is the gradient through the thickness. As it

cannot be reduced much due to the low through-plane thermal conductivity of the cell.

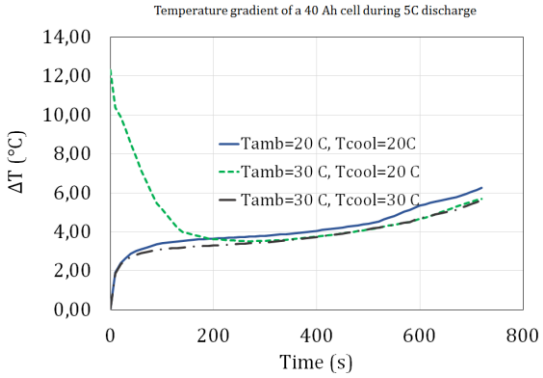

Figure 10. Volumetric temperature gradient of the 40 Ah cell at 20 °C and 30 °C ambient temperature under 5C discharge. The water/glycol velocity is equal to V=0.5 m/s for all the cases.

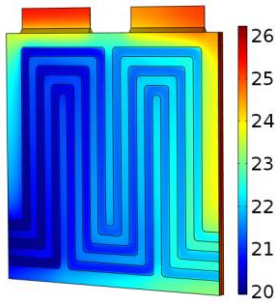

Figure 11. Temperature distribution of a 40 Ah cell at the end of 5C discharge at 20°C ambient temperature with water/glycol mixture coolant, V=0.5 m/s.

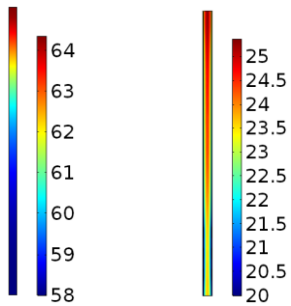

Figure 12. Temperature distribution of a 40 Ah cell through the cell thickness at the end of 5C discharge at 20°C ambient temperature, (a) with no cooling, (b) with water/glycol mixture coolant, V=0.5 m/s.

4 Conclusion

This study indicates impact of cell size on the heat generation and temperature distribution of the cell, which has a high influence on the battery aging. Large format batteries have high packing efficiency, but on the other hand they have a large temperature gradient, which is the main concern for their application. Having such a temperature gradient requires a more complex cooling design. On the other hand, having small capacity batteries leads to a large number of cells in a pack while it benefits from a simple cooling design.

In this study an electrochemical-thermal model was developed to investigate the temperature distribution of a 10 Ah, 20 Ah and 40 Ah LFP pouch cell applying two cooling strategies: fin cooling and indirect liquid cooling. The simulation results show that the aluminium plate is not an effective cooling method when having large format cells. Even though it can reduce the average temperature of the cells, it is unable to decrease the temperature gradient of the cells effectively. For the 10 Ah, operating under 3C, with $t_{Al} = 1.5\ mm$ and $t_{Al} = 5\ mm$, the temperature gradient of the cell decreased to 12 °C and 5 °C respectively. However, inserting a $5\ mm$ plate between each two cells adds extra weight to the system which is not desirable. But for $t_{Al} = 1.5\ mm$ by modifying the fin design, there is a potential for effective cooling of the 10 Ah cell operating under 3C, which is the case in most vehicle application.

The second approach involved employing an indirect liquid cooling method, with a total plate thickness of $1.5\ mm$. Water/glycol mixture and mineral oil were applied as the coolants. The simulation results shows that both the temperature gradient and average temperature of the battery reduced significantly applying the water glycol mixture whereas the mineral oil indicated a larger temperature gradient and higher average temperature. Moreover, the pressure drop of the mineral oil in a cooling channel was significantly higher than that of the water/glycol mixture, which means a higher parasitic power is required in case of oil cooling.

The most important highlight of this study is that, the limiting factor for reducing the volumetric temperature gradient of the cell is the gradient through the thickness, which is limited by the low through-plane thermal conductivity of the cell. It means that in case of having a thick cell, by applying surface cooling methods for cells under high levels of internal heat generation, it is quite

difficult to reach a temperature gradient of below 5°C, no matter how efficient a cooling system is.

Acknowledgments

The research within this paper is undertaken as a part of ELEVATE (EP/M009394/1) and APC Spoke Institutional Sponsorship projects (EP/P511432/1) funded by the Engineering and Physical Science Research Council (EPSRC).

References

[1] D. Chen, J. Jiang, G. H. Kim, C. Yang, and A. Pesaran, *Comparison of different cooling methods for lithium ion battery cells*, Journal of Applied Thermal Engineering, 94(2016), 846–854

[2] A. Greco, X. Jiang, and D. Cao, *An investigation of lithium-ion battery thermal management using paraffin/porous-graphite-matrix composite*, Journal of Power Sources, 278(2015), 50–68

[3] R. Zhao, J. Gu, and J. Liu, *An experimental study of heat pipe thermal management system with wet cooling method for lithium ion batteries*, Journal of Power Sources, 273(2015), 1089–1097

[4] A. A. Pesaran, *Battery thermal models for hybrid vehicle simulations*, Journal of Power Sources, 110(2002), 377–382

[5] H. Teng and K. Yeow, *Design of Direct and Indirect Liquid Cooling Systems for High-Capacity, High-Power Lithium-Ion Battery Packs*, SAE Tech-2012.

[6] G. Karimi and X. Li, *Thermal management of lithium-ion batteries for electric vehicles*, International Journal of Energy Research, 37(2013), 13-24

[7] A. A. Pesaran, S. Burch, and M. Keyser, *An approach for designing thermal management systems for electric and hybrid vehicle battery packs*, The Fourth Vehicle Thermal Management Systems Conference and Exhibition, 1999

[8] N. Yang, X. Zhang, G. Li, and D. Hua, *Assessment of the forced air-cooling performance for cylindrical lithium-ion battery packs: A comparative analysis between aligned and staggered cell arrangements*, Journal of Applied Thermal Engineering, 80(2015), 55–65

[9] L. Fan, J. M. Khodadadi, and A. A. Pesaran, *A parametric study on thermal management of an air-cooled lithium-ion battery module for plug-in hybrid electric vehicles*, Journal of Power Sources, 238(2013), 301–312

[10] T. Wang, K. J. Tseng, J. Zhao, and Z. Wei, *Thermal investigation of lithium-ion battery module with different cell arrangement structures and forced air-cooling strategies*, Journal of Applied Energy, 134(2014), 229–238

[11] Y. Ma, H. Teng, and M. Thelliez, Electro-*Thermal Modeling of a Lithium-ion Battery System*, 3(2016), 306–317

[12] T. Wang, K. J. Tseng, and J. Zhao, *Development of efficient air-cooling strategies for lithium-ion battery module based on empirical heat source model*, Journal of Appllied Thermal Engineering, 90(2015), 521–529

[13] D. C. Erb, I. M. Ehrenberg, S. E. Sarma, and E. Carlson, *Effects of cell geometry on thermal management in air-cooled battery packs*, IEEE-2015

[14] W. Tong, K. Somasundaram, E. Birgersson, A. S. Mujumdar, and C. Yap, *Numerical investigation of water cooling for a lithium-ion bipolar battery pack*, International Journal of Thermal Sciences, 94(2015), 259–269

[15] Y. Ye, L. H. Saw, Y. Shi, and A. A. O. Tay, *Numerical analyses on optimizing a heat pipe thermal management system for lithium-ion batteries during fast charging*, Journal of Applied Thermal Engineering, 86(2015), 281–291

[16] Q. Wang, B. Jiang, Q. F. Xue, H. L. Sun, B. Li, H. M. Zou, and Y. Y. Yan, *Experimental investigation on EV battery cooling and heating by heat pipes*, Journal of Applied Thermal Engineering, 88(2014), 54–60

[17] T. H. Tran, S. Harmand, B. Desmet, and S. Filangi, *Experimental investigation on the feasibility of heat pipe cooling for HEV/EV lithium-ion battery*, Journal of Applied Thermal Engineering, 63(2014), 551–558

[18] R. Sabbah, R. Kizilel, J. R. Selman, and S. Al-Hallaj, *Active (air-cooled) vs. passive (phase change material) thermal management of high power lithium-ion packs: Limitation of temperature rise and uniformity of temperature distribution*, Journal of Power Sources, 182(2008), 630–638

[19] Z. Rao, S. Wang, and G. Zhang, *Simulation and experiment of thermal energy management with phase change material for ageing LiFePO 4 power battery*, Journal of Energy Conversion and Management, 52(2011), 3408–3414

[20] Z. Rao, Q. Wang, and C. Huang, *Investigation of the thermal performance of phase change material/mini-channel coupled battery thermal management system*, Journal of Applied Energy, 164(2016), 659–669

[21] Z. Rao and S. Wang, *A review of power battery thermal energy management*, Renewable and Sustainable Energy Reviews., 15(2011), 4554–4571

[22] T. M. Bandhauer, S. Garimella, and T. F. Fuller, *A Critical Review of Thermal Issues in Lithium-Ion Batteries*, Journal of Electrochemical Society, 158(2011), R1-R25

[23] A. Pesaran, *Battery Thermal Management in EVs and HEVs : Issues and Solutions*, Advanced Automotive Battery Conference, 2001.

[24] D. Worwood, E. Hosseinzadeh, K. Q, J. Marco, D. Greenwood, M. R, W. . Widanage, A. Barai, and P. Jennings, Thermal analysis of a lithium-ion pouch cell under aggressive automotive duty cycles with minimal cooling, IET Hybrid Electr. Veh. Conf., HEVC-2016.

Authors

Dr Elham Hosseinzadeh received her PhD in Feb 2013 from Technical University of Denmark (DTU), with focus on "Modelling and Design of Hybrid PEM Fuel Cell Systems for Lift Trucks". After completion of her PhD, she worked for IRD Fuel cell company as a Research Engineer for a couple of years. She has joined Warwick Manufacturing Group (WMG) as a research fellow in Jan 2016. She is currently working on electrochemical modelling of lithium ion batteries as well as battery thermal management.

Dr Anup Barai has a PhD degree from University of Warwick, a First-Class MSc degree in Embedded Systems Design and a BSc (Honours) degree in Electrical and Electronic Engineering. Anup has been working at WMG since 2011, currently as a research fellow. Since joining WMG Anup has delivered research which has tangible impact on industrial and academic researcher's success, making fundamental changes in the way energy storage systems are characterised.

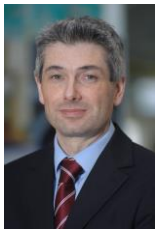

Dr James Marco is a Chartered Engineer and a member of the Institution of Engineering and Technology (MIET). After graduating with an Engineering Doctorate from Warwick in 2000, he worked for several years within the automotive industry. Research interests include systems engineering, real-time control, systems modelling, design optimisation and the design of battery management and energy management control systems.

Paul Jennings received a BA degree in physics from the University of Oxford in 1985 and an Engineering Doctorate from the University of Warwick in 1996. Since 1988 he has worked on industry-focused research for WMG at the University of Warwick. His current interests include: vehicle electrification, in particular energy management and storage; connected and autonomous vehicles, in particular the evaluation of their dependability; and user engagement in product and environment design, with a particular focus on automotive applications.